HYDRAULICS AND FLOOD FLOW STRUCTURES OF RIPARIAN-VEGETATED MEANDERING CHANNELS

Z. Ibrahim[1], Z. Ismail[1], S. Harun[1], K. Shiono[2], N. M. Zuki[1], M. R. Makhtar[1], M. S. A. Rahman[1] and M. H. Jamal[1]

[1]Department of Hydraulics and Hydrology, Faculty of Civil Engineering, Universiti Teknologi Malaysia (UTM). 81310 UTM Johor Bahru, Johor, Malaysia.
E-mail: zulkfe@utm.my
[2]Department of Civil and Building Engineering, Loughborough University, Leicestershire, United Kingdom.

Floods are frequent natural disasters occur in every part of the globe. The recent floods in the Malaysian states including Kelantan, Pahang, Terengganu, Perak, Sabah and Johor have damaged the residential properties, infrastructures and crops or even deaths. Removal of vegetation or trees on the floodplains has been pointed out as one of contributing factors to the severity of damages. It is essential to understand the influence of floodplain vegetation on the river hydraulics during flooding. The behaviours of overbank flows in non-mobile bed vegetated meandering channel were investigated in the laboratory utilizing a scale physical model. Two-lined 5 mm diameter steel rods were installed in staggered arrays for very close rod spacing along the riparian zone to simulate as emergent floodplain vegetation. Attentions were given to stage-discharge relationship, flow resistance, depth-averaged velocity distribution and horizontal vorticity patterns in the vegetated and non-vegetated compound channels. This paper discusses the hydraulics of non-mobile bed meandering channels during shallow and deep flood flow inundations. The findings showed that riparian vegetation had significant effects on the compound meandering channel hydraulics.

Keywords: Laboratory Experiment, Riparian Vegetation, Meandering Channel, Flood, Flow Structure

1. Introduction

Floods are becoming frequent natural disaster in many part of the globe. Disaster statistics in Malaysia between 1980 to 2010 shows that 85.4% of people in Malaysia are flood affected and the figure is the highest percentage (*http://*www.preventionweb.net/english/countries/statistics*)*. The recent floods in the Malaysian states including Kelantan, Pahang, Terengganu, Perak, Sabah and Johor have damaged the residential properties, infrastructures and crops or even deaths. Deforestation including removal of floodplain vegetation (trees) has been pointed out as one of contributing factors to the severity of damages. Therefore, it is essential to understand the influence of floodplain or riparian vegetation on the flooded river hydraulics.

Rivers can be classified as straight, meandering and braiding (Leopold and Wolman, 1957) and meandering is the most common planform acquired by natural rivers. The meandering channel flow is considerably more complex and unique than straight channel. Muar River is the most sinuous Malaysian river in Malaysia with the sinuosity of 4.056 while the average sinuosity of Malaysian rivers is about 1.54 (Ibrahim, *et al.*, 2012; Ibrahim, 2015). Field work is difficult under flood conditions when data acquisition is difficult and sometimes dangerous (Myers *et al*., 1999). Among the recent experimental researches on vegetated compound meandering channels flows were Ismail and Shiono (2006), Ismail (2007) and Jahra *et al.* (2010). The understanding on the hydraulics of compound or flooded meandering channels with closed spaced riparian vegetation is still need to be explored.

Regarding to the problem, a research was conducted to study the flood flow characteristics in non-mobile bed compound meandering channels for non-vegetated and riparian vegetated cases. The focus was given to stage-discharge relationship, flow resistance, streamwise velocity distribution and horizontal vorticity patterns in the channels. The flume experiment or simulation was conducted in the Hydraulics Laboratory in Universiti Teknologi Malaysia (UTM). The flood flow characteristics were focused on the shallow and deep flood flow conditions.

Experimental Research

The experimental research was carried out in a non-mobile bed meandering channel constructed in a 12 m long and 3 m wide flume which consisted of a main channel and two floodplains on its sides. A 0.5 m wide meandering channel with sinuosity of 1.54 was constructed in the flume as illustrated in Figure 1(a). The channel wave length and meander belt width were 3.4 m and 2.2 m, respectively. The geometrical parameters were main channel width, B_{mc} = 0.5 m and depth, H_{mc} = 0.1 m as shown in Figure 1(b). The channel was made of rigid boundary type of cross section and flume bed was fixed at a gradient of 0.1%. Two-lined 5 mm diameter steel rods were installed in staggered arrays along the riparian zone to simulate as emergent vegetation with a very close 2d spacing where d represented the rod diameter.

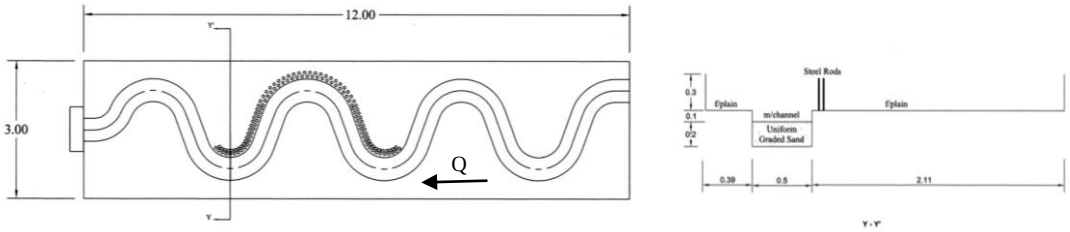

(a) Plan view (b) Cross-sectional view

Figure 1: Riparian vegetated meandering compound channel

The re-circulating flume system was used and flow rate or was measured using a portable flow meter. A digital water surface profiler or point gauge was utilized for flow depth measurement along the main channel and water depth was controlled by downstream tailgates. Measurements were carried out once the maximum difference between water surface and bed slopes was 5% as "quasi-uniform" flow had been achieved (Sun and Shiono, 2009).

The 3D velocity was measured using a Vectrino^{+} Acoustic Doppler Velocimeter (ADV) with a sampling rate of 100 Hz. The minimum recording time for each point velocity was 60 s. The data collection equipments were placed on a mobile carriageway. Principally, the ADV measures the 3D velocities (U, V, W) of water particles located 5 cm below its probe (Nortek, 2004). The measurement sections located 7 m downstream of channel inlet with a longitudinal distance of half wave length, namely sections S1, S8, and S15 as depicted in Figure 2. The sections S1 and S15 were the upstream and downstream apices and S8 was the crossover section. The velocities were measured every 2 cm in transverse direction at several vertical layers.

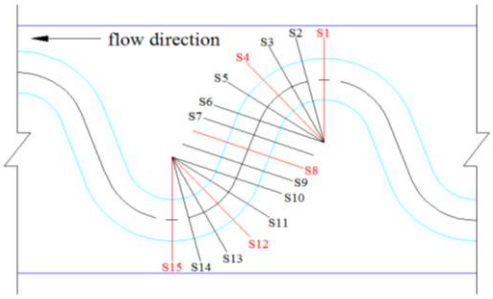

Figure 2: Layout plan of data measurement sections

Results and Discussion

Stage-Discharge

The flooding flow velocities are measured at relative depths or depth ratios (DR) of 0.30 (shallow) and 0.45 (deep). The relative depth is calculated as ratio of floodplain flow depth to total flow depth. Using recorded maximum velocities at apices gives the experimental Reynolds numbers larger than 27,000 while Froude numbers are from 0.14 to 0.25, indicates that turbulent-subcritical flows take place in the meandering channel.

Figures 3 and 4 depict stage (H)-discharge (Q) and DR-Q relationships for non-vegetated (NV) and riparian vegetated (2d) channels. The flows in the channel are inbank, bankfull and overbank. The 100 mm flow depth is the bankfull level and discharge to initiate overbank flow in the channel is 17 L/s. It can be seen in Figure 3 that the maximum H for 2d vegetated case increases by 32% compared to non-vegetated case. This is due to the flow retardation effect by the floodplain vegetation in the meandering channel. This effect can also be visualized in Figure 4 where the resulted maximum DRs for vegetated and non-vegetated cases are 0.57 and 0.45, respectively.

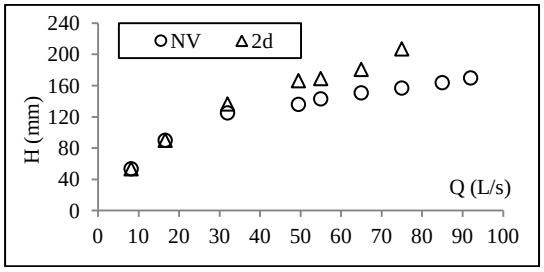

Figure 3: H-Q relationship

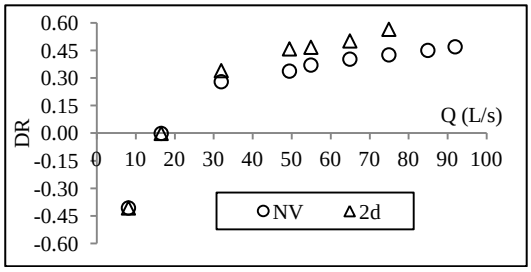

Figure 4: DR-Q relationship

Manning's n

The flow resistance is represented by Manning's *n*. The experimental Manning's *n* is calculated from the earlier H-Q data. The typical Manning's equation as given in Equation (1) is applied to determine the composite *n* of compound meandering channel.

$$n = \frac{A\,R^{2/3}\,\sqrt{S_o}}{Q} \qquad (1)$$

Figure 5 displays the Manning's *n* for the two cases at various DR in the meandering channels. The *n* for non-vegetated increases as flow changes from inbank to overbank and the roughness value represents the resistance due to the channel surface itself. The result shows *n* increases with relative depth which it is also means that it increases with discharge in the channel. The *n* value increases from 0.012 to

0.013 as the inbank flow shifts to bankfull in meandering channel. Subsequently, *n* value increases as overbank flow occurs in the channel. The flow resistance coefficient increases to 0.016 and almost uniform for overbank cases. In the case of overbank flow, Manning's *n* varies and becomes constant as relative depth reaches 0.40.

However, the Manning's *n* for vegetated cases keep increasing as channel flow depth increases. The 2d rod case exhibits the maximum Manning's *n* value of 0.033 at DR of 0.57. Flow resistance in flooding riparian vegetated meandering channels is larger than non-vegetated. Value of *n* is highly variable and influential factors including surface roughness, vegetation, channel alignment and channel irregularity (Chow, 1959; Sturm, 2001).

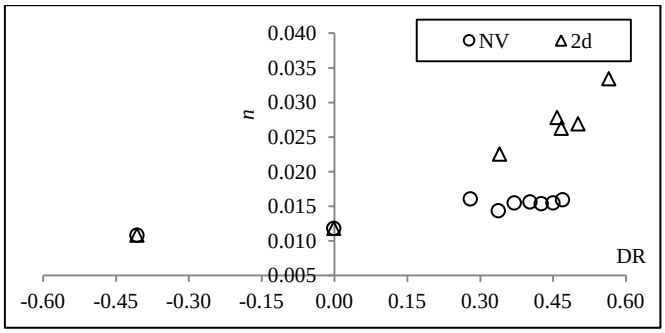

Figure 5: Relative Depth, *DR* against Manning's *n*

Depth-averaged Velocity Distribution

In order to understand the flow properties in meandering channels, 3D velocity (U, V, W) are measured using the ADV across sections S1, S8 and S15 (see Figure 2). The analyzed temporal-averaged velocity components are used to plot the spatial distribution across each section. The depth-averaged or depth-mean velocity U_d is computed using Equation (2) where the streamwise velocity is averaged over the flow depth. Figures 6 and 7 illustrate the transverse distributions of depth-averaged velocity U_d in compound meandering channels for relative depths of 0.30 and 0.45, respectively.

$$U_{d(y)} = \frac{1}{H(y)} \int_0^{H(y)} U dz \qquad (2)$$

The left hand side (LHS) floodplain is located between y = 0 to 20 cm; main channel is situated between y = 20 to 70 cm and location of right hand side (RHS) floodplain is between y = 70 cm to 90 cm. In shallow flow depth as presented in Figure 6, it is observed that most of the flow takes place in the main channel. The riparian vegetation at section S8 has forced the flow to concentrate in the main channel and no flow is allowed in the RHS floodplain for vegetated cases. It can also be seen that the maximum U_d shifts from LHS inner bend at upstream apex S1 to RHS inner bend at downstream apex S15. This feature is opposite to the inbank flow characteristics, as mentioned in Willetts and Rameshwaren (1996) and Shiono *et al.* (2008).

Figure 7 shows that when the relative depth rises to 0.45, the flow is distributed more uniform between main channel and floodplains particularly for non-vegetated case. The velocity in RHS floodplain is always small due to the presence of the riparian vegetation or rods and it is similar to observation by Jahra *et al.* (2010). On the other hand, its magnitude increases as compared to a lower relative depth case. It

is noted that U_d in main channel and LHS floodplain for vegetated case at S15 (Figure 7(c)) is almost equal to or higher than U_d values in non-vegetated case because their locations are not influenced by riparian vegetation on RHS floodplain. The depth-averaged velocity distributions show the presence of shear layers in main channel-floodplain interface zones which is a common feature in compound channels.

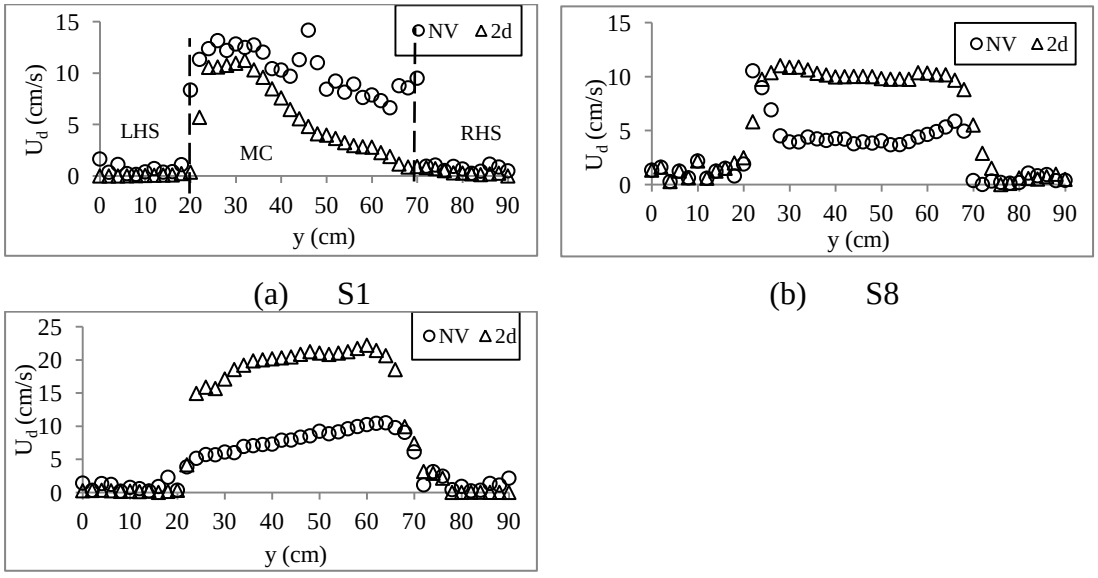

(a) S1 (b) S8

(c) S15

Figure 6: Transverse distribution of experimental depth-averaged velocity, U_d along the meandering channel for low relative depth of 0.30

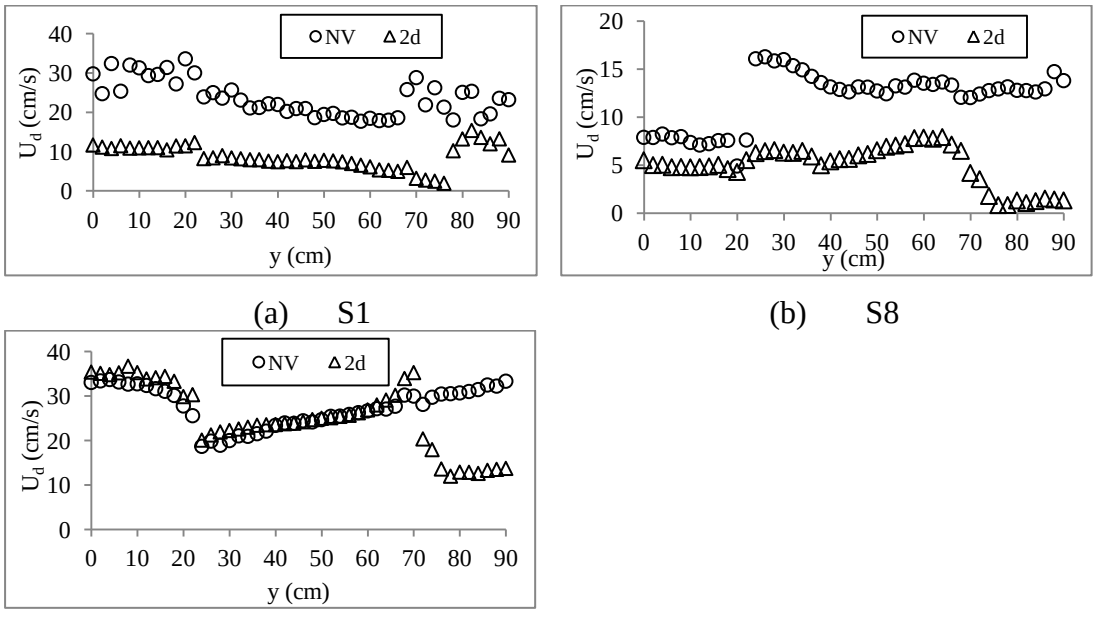

(a) S1 (b) S8

(c) S15

Figure 7: Transverse distribution of experimental depth-averaged velocity U_d along the meandering channel for high relative depth of 0.45

Horizontal Vorticity

The horizontal secondary flow or circulation is also known as "stream-wise vorticity" (Tang and Knight, 2009; Sanjou and Nezu, 2009; Tominaga and Nezu, 1991). Figures 8 and 9 present the normalised vorticity patterns at sections S1, S8 and S15 for both flood depths in the non-vegetated meandering channels. Symbols y, z H and U_s represent the lateral distance, vertical distance, total flow depth and mean sectional streamwise velocity in the channel, respectively.

The circulation pattern at section S1 in Figure 8 does not clearly display the main channel-floodplain flows interaction due to shallow flood depth but anti-clockwise internal circulation is observed in LHS main channel corner (or inner bend). Meanwhile, two secondary current cells present in crossover section S8. In contrast, the secondary flow direction changes at section S15 where clockwise internal flow is seen in the RHS corner (inner bend) of the main channel. In general, the stronger secondary currents occur at bottom flow layer at apices. The secondary flows are due to shear-generated turbulence and centrifugal force in the channel (Shiono and Muto, 1998).

Deeper flood flow in Figure 9 shows stronger secondary currents between floodplains and main channel takes place especially in upper flow layers at crossover section S8. This demonstrates the plunging of floodplain flow into main channel and expulsion of main channel flow into floodplain, mentioned as flood mechanism in Willetts and Hardwick (1993). Turbulence-generated by floodplain flow crossing the main channel is greater than bed-generated turbulence (Shiono *et al.*, 2008). Similar results obtained by Muto and Ishigaki (1999) which stated that secondary flow cell became larger as the flood depth rose and flood flow structure was controlled by flow interaction at crossover. Opposite direction internal circulations generated by bend centrifugal force take place at both apices S1 and S15.

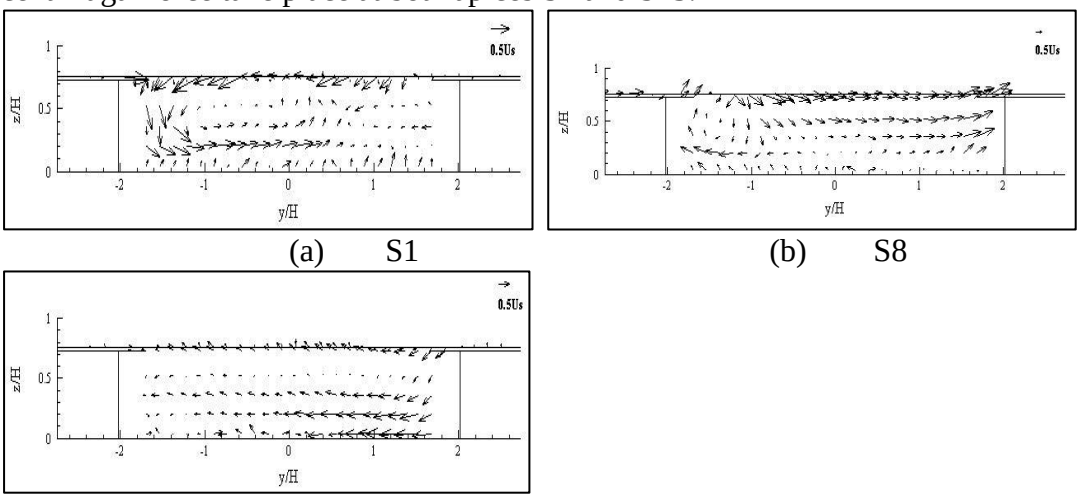

(a) S1 (b) S8

(c) S15

Figure 8: Secondary flows in a non-vegetated meandering channel for relative depth of 0.30

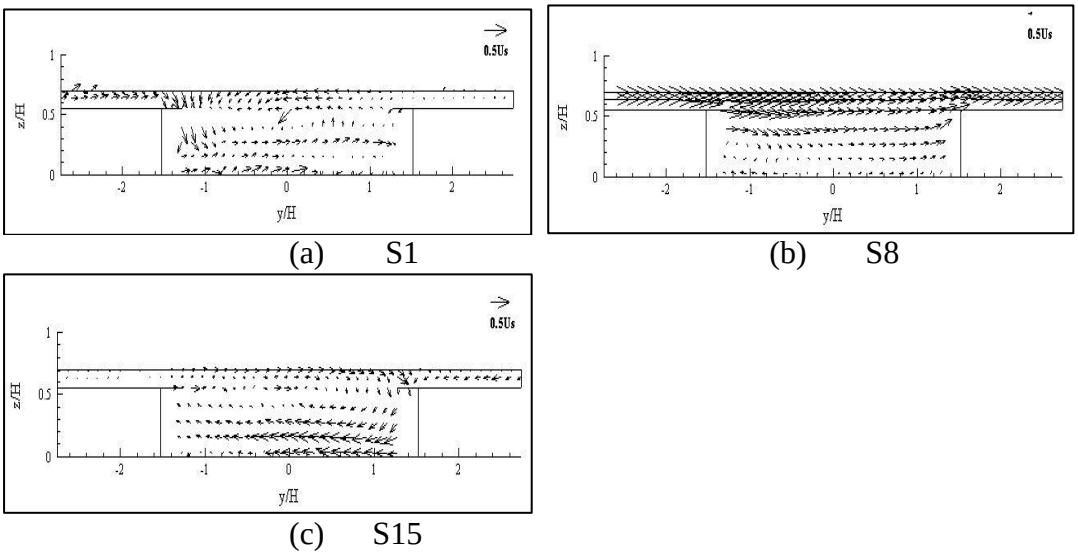

(a) S1 (b) S8

(c) S15

Figure 9: Secondary flows in a non-vegetated meandering channel for relative depth of 0.45

The current patterns for 2d spacing riparian vegetation for low DR of 0.30 are displayed in Figure 10. In general, the current patterns are similar to what are shown in Figure 8 in non-vegetated case. However, the riparian vegetation has restricted the main channel flow to enter the RHS floodplain at S8. Internal circulations at apices S1 and S15 are strong but in opposite directions.

Circulations for DR of 0.45 are illustrated in Figure 11, it can be seen that floodplain-main channel flows interaction becomes stronger and intensified particularly at S8. Internal vortices also develop in the mid-depth and lower flow layers at channel crossover S8. Apparently, these internal vortices present in the lower flow layers at S1 and S15, which is a typical apices secondary flow structure. Muto and Ishigaki (1999) and Ismail (2007) found that vegetation limited and retarded upper flow layer. Naish and Sellin (1996) reported that secondary flow cells became stronger for high flow depth. Thus the experimental results are in agreement to earlier research findings.

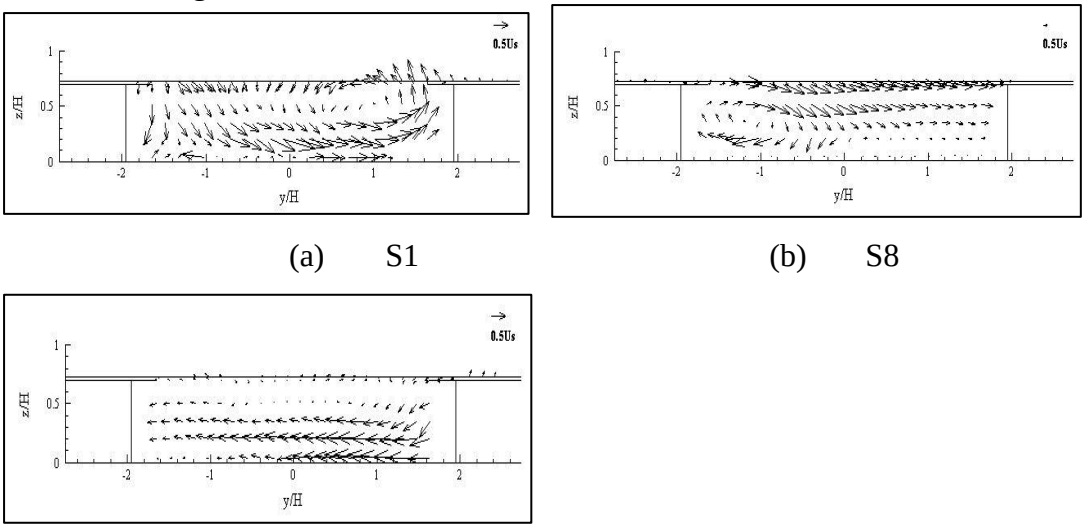

(a) S1 (b) S8

(c) S15

Figure 10: Secondary flows in riparian vegetated meandering channel for relative depth of 0.30

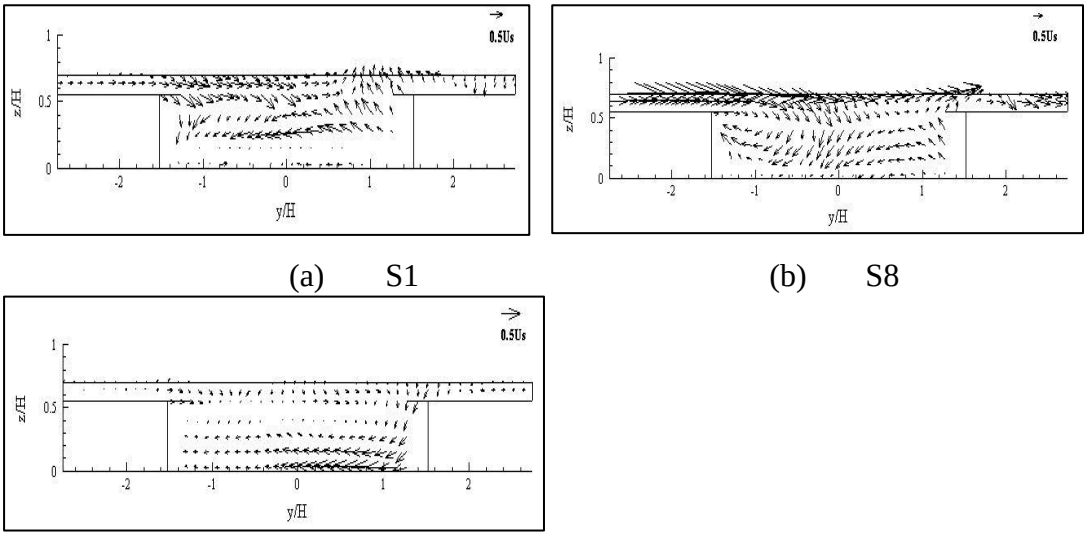

(a) S1 (b) S8

(c) S15

Figure 11: Secondary flows in riparian vegetated meandering channel for relative depth of 0.45

Conclusions

The hydraulics of riparian vegetated and non-vegetated non-mobile bed meandering channel for shallow and deep overbank flows have been investigated through flume simulations. The findings of the experimental study are: (i) riparian vegetation increase flood flow depth in main channel due to flow retardation effect, (ii) riparian vegetation also increases the channel flow resistance and rises in deeper flood, (iii) depth-averaged velocity distribution is vegetation and flow depth-influenced, and the pattern varies along the meandering channel, and (iv) turbulence and centrifugal force-generated secondary flows are observed in the compound meandering channel and stronger main channel-floodplain flows interaction takes place in the channel crossover during high flood but the flow is controlled by riparian vegetation.

Acknowledgement

The financial of this research is supported by the Research Management Centre (RMC), UTM under Research University Grant vote no. 03J97. The authors are indebted to other UTM Faculty of Civil Engineering students involved in the study for their assistance during the experimental work.

References

Chow, V. T. (1959). *Open-Channel Hydraulics*. Singapore: McGraw-Hill.

Ibrahim, Z. (2015). *Flow behaviour due to floodplain roughness along riparian zone in compound channels.* Universiti Teknologi Malaysia. PhD Thesis.

Ibrahim, Z., Ismail, Z., Harun, S., Kalimuddin, N.M., Makhtar, M.R. and Yunus, T. N. T. (2012). *Flood flow characteristics in non-vegetated meandering channel: A flume simulation.* Proc. International Conference on Water Resources (ICWR 2012), Langkawi. 5-6 November. 31-39.

Ismail, Z. and Shiono, K. (2006). The effect of vegetation along cross-over floodplain edges on stage-discharge, sediment transport rates in compound meandering

channels. *Proc. of 5th WSEAS Int. Conf. on Env. Ecosystem & Development.* Venice. 407-412.

Ismail, Z. (2007). *A Study of overbank flows in non-vegetated and vegetated floodplains in compound meandering channels.* Ph.D Thesis, Loughborough University, U.K.

Ismail, Z. and Shiono, K. (2007). The behaviour of stage-discharge, flow resistance and sediment transport influenced by floodplain roughness. *5th Int. Symp. On Env. Hydraulics, Arizona,* CD ROM.

Jahra, F., Yamamoto, H., Tsubaki, R. and Kawahara. Y. (2010). Turbulent flow structure in meandering vegetated open channel. *River Flow 2010*. 153-161.

Leopold, L.B. and Wolman, M.G. (1957) River channel patterns: braided, meandering and straight. U.S. Geological Survey Professional Paper 282-B. 39-85.

Muto, Y. and Ishigaki, T. (1999). Secondary flow in compound sinuous/meandering channels. In Rodi, W. and D. Laurence, D. (Eds.) *Engineering Turbulence Modelling and Experiments –4*. Elsevier Science Ltd. 511-520.

Myers, W.R.C., Knight, D.W., Lyness, J.F., Cassells, J.B. and Brown, F. (1999) Resistance coefficients for inbank and overbank flows. *Proc. Instn. Wat. Marit. & Energy*, 136 (6): 105-115.

Naish, C. and Sellin, R.H.J. (1996). Flow structure in a large-scale model of a doubly meandering compound river channel. In Ashworth, Bennett, Best and McLelland (Eds.). *Coherent Flow Structures in Open Channel*. New York: John Wiley and Sons. 631-654.

Nortek AS. (2004). *Vectrino velocimeter user guide*.

Sanjou, M. and Nezu, I. (2009). *Turbulence structure and coherent motion in meandering compound open-channel flows. J. Hydr. Research*. 47(5): 598-610.

Sturm, T.W. (2001). *Open Channel Hydraulics.* Singapore: McGraw Hill.

Shiono, K., Spooner, J., Chan, T., Rameshwaran, P. and Chandler, J. (2008). Flow characteristics in meandering channels with non-mobile and mobile beds for overbank flows. *J. of Hydraulic Research*. 46(1): 113-132.

Shiono, K. and Muto, Y. (1998). Complex flow mechanism in compound meandering channels with overbank flow. *J. Fluid Mech*. 376: 221-261.

Sun, X. and Shiono, K. (2009). Flow resistance of one-line emergent vegetation along the floodplain edge of a compound open channel. *J. in Advances Water Resources*. 32 (3): 430-438.

Tang, X. and Knight, D.W. (2009). Analytical models for velocity distributions in open channel flows. *J. of Hydraulic Research.* 47(4): 418-428.

Tominaga, A. and Nezu, I. (1991). Turbulent structure in compound open channels. *J. of Hydraulic Engineering*. 117(1): 21-41.

Willetts, B.B. and Rameshwaran, P. (1996). Meandering overbank flow structures. In Ashworth, Bennett, Best and McLelland (Eds.). *Coherent Flow Structures in Open Channel*. New York: John Wiley and Sons. 609-629.

Willetts, B.B. and Hardwick, R.I. (1993). Stage dependency for overbank flow in meandering channels. *Proc. Instn. Civ. Engrs. Wat. Marit. & Energy*. 101(3): 45-54.

http://www.preventionweb.net/english/countries/statistics.